Altered resting-state effective connectivity of fronto-parietal motor control systems on the primary motor network following stroke

Cory S. Inman[1], **G. Andrew James, PhD**[2], **Stephan Hamann, PhD**[1], **Justin K. Rajendra**[4], **Giuseppe Pagnoni, PhD**[3], and **Andrew J. Butler, PhD, PT FAHA**[4,5]

[1]Department of Psychology, Emory University, Atlanta, GA 30322

[2]Psychiatric Research Institute, University of Arkansas for Medical Sciences, Little Rock, AR, USA

[3]Department of Biomedical Sciences, University of Modena and Reggio Emilia, Modena, Italy

[4]Department of Rehabilitation Medicine, School of Medicine, Emory University, Atlanta, GA 30322

[5]Rehabilitation R&D Center of Excellence, Atlanta VAMC, Decatur, GA, 30322, USA

Abstract

Previous brain imaging work suggests that stroke alters the effective connectivity (the influence neural regions exert upon each other) of motor execution networks. The present study examines the intrinsic effective connectivity of top-down motor control in stroke survivors (n=13) relative to healthy participants (n=12). Stroke survivors exhibited significant deficits in motor function, as assessed by the Fugl-Meyer Motor Assessment. We used structural equation modeling (SEM) of resting-state fMRI data to investigate the relationship between motor deficits and the intrinsic effective connectivity between brain regions involved in motor control and motor execution. An exploratory adaptation of SEM determined the optimal model of motor execution effective connectivity in healthy participants, and confirmatory SEM assessed stroke survivors' fit to that model. We observed alterations in spontaneous resting-state effective connectivity from fronto-parietal guidance systems to the motor network in stroke survivors. More specifically, diminished connectivity was found in connections from the superior parietal cortex to primary motor cortex and supplementary motor cortex. Furthermore, the paths demonstrated large individual variance in stroke survivors but less variance in healthy participants. These findings suggest that characterizing the deficits in resting-state connectivity of top-down processes in stroke survivors may help optimize cognitive and physical rehabilitation therapies by individually targeting specific neural pathway.

Keywords

Exploratory Structural Equation Modeling; Functional imaging; Motor circuits; Network Analysis; Top-Down Control

Correspondence to Cory Inman, Department of Psychology, Emory University or Andrew J. Butler, PhD, PT, Department of Rehabilitation Medicine, School of Medicine, Emory University, Atlanta, GA USA, 36 Eagle Row, Atlanta, GA 30033, Phone: 404-727-6304, Fax: 404-727-0372, corysinman@gmail.com or Andrew.Butler@emory.edu.

Publisher's Disclaimer: This is a PDF file of an unedited manuscript that has been accepted for publication. As a service to our customers we are providing this early version of the manuscript. The manuscript will undergo copyediting, typesetting, and review of the resulting proof before it is published in its final citable form. Please note that during the production process errors may be discovered which could affect the content, and all legal disclaimers that apply to the journal pertain.

1. Introduction

Stroke is the leading cause of severe, long-term disability in the United States (Rosamond, Flegal, Friday, et al, 2007). More than 1.1 million Americans report difficulty with functional limitations in daily life following stroke. Impairment and functional limitations can range from mild to severe, depending on several factors, including stroke location and extent of lesion (CDC, 1999). The physical impairments experienced by stroke survivors have a profoundly negative impact on their daily activities and quality of life.

Functional neuroimaging has improved our understanding of the pathophysiology of stroke by identifying the neuroanatomic components of the human motor system (Passingham, 1987; Deiber, Passingham, Colebatch, et al., 1991; Tanji, 1996; Yousry, Schmid, Alkadhi, 1997; Rijntjes, Buechel, Kiebel, and Weiller, 1999; Liu, Pu, Gao, Parsons, et al., 2001) and elucidating the complex, dynamic neural interactions underlying task-related motor function (Miyachi, Hikosaka, Miyashita, Kárádi, et al., 1997; Toni, Krams, Turner, and Passingham, 1998; Cabeza and Nyberg, 2000; Liu, Ramnani, Toni, Passingham, and Haggard, 2001). Causal modeling has further enhanced our understanding of neuroanatomy by modeling dynamical interactions within a network of regions of interest rather than activity in individual brain regions. The emphasis thereby changes from the influence of individual brain regions active in each condition to the influence neural regions have upon each other, an aspect of brain function known as effective connectivity (McIntosh and Gonzalez-Lima, 1994; Buchel and Friston, 1997; Buchel, Coull, and Friston, 1999; Friston, Harrison, and Penny, 2003). In their pioneering study, Solodkin et al. (Solodkin, Hlustik, et al., 2004) used structural equation modeling (SEM) to assess motor network activation during motor execution, visual imagery, and kinesthetic imagery in healthy volunteers. They demonstrated that motor imagery and motor execution were associated with remarkably similar brain networks. With regard to the present study, data from Solodkin et al. provide an established template of the motor imagery/execution network upon which to establish comparisons between the same motor execution networks in healthy individuals and stroke survivors with known motor deficits.

Solodkin and colleagues (Solokin, Hlustik, et al., 2004) used available information about the anatomical connections and physiology of the cortical motor system in macaques to build a *confirmatory* model of effective connectivity in humans. While this approach is valid, it assumes a direct and complete correspondence between anatomy and function. However, while anatomic connectivity may exist between two neural regions, it is not necessary or sufficient for functional or effective connectivity, because of the potential involvement of other driving regions or due to well-documented task-dependent modulations of the functional relationship of the regions' activity (Toni et al., 1998; He, Tan, Tang, James, et al., 2003; Grefkes, Eickhoff, Nowak, et al., 2008b). Thus, in the present study we propose using an exhaustive exploratory variation of SEM that tests all possible models connecting a set of specified regions (Zhuang, LaConte, Peltier, et al., 2005; James, Mayberg, Hu, et al., 2009b).

The confirmatory approach to SEM is beneficial for initial descriptions of effective connectivity with a given data set, but is limited by the need to make educated *a priori* predictions of best-fitting models for a given dataset, thereby restricting models to theoretically driven paths. While adjusting the model to one's data is possible, the process becomes intractable when considering all possible adjustments that could be made. For data-driven characterizations of connectivity iterative, exploratory approaches are needed. In the current study, exploratory SEM allows us to characterize the best model for our prescribed regions of interest (ROIs) in healthy controls before applying this model to a dataset of

stroke survivors. This approach is advantageous because it allows researchers to assess the relative integrity of motor execution networks in stroke survivors compared to that of healthy individuals.

Structural equation modeling is a well-established technique for assessing causal influences for both psychological and biomedical research. SEM infers causality by gauging whether a proposed model is supported by the covariance observed within the data. SEM differs from autoregressive techniques such as Granger causality and dynamic causal modeling, which directly estimate causality by gauging if past values of a variable reliably predict its current value, and if the predictive value improves with inclusion of past values of other variables. We propose that SEM is better suited for analysis of resting-state BOLD than autoregressive techniques, given the spontaneous, cyclic nature of resting-state BOLD and the absence of structured "starting-points" indicating influence on cognitive tasks.

A confound to assessment of brain function in stroke survivors is that motor impairments escalate task difficulty – i.e. a 1 Hz finger tapping task may be trivial for an able-bodied participant but require more effort for a stroke survivor using his or her hemiparietic hand. Fortunately, several functionally distinct neural networks exhibit coordinated activity during the performance of a task as well as during rest (Fox, Snyder, Vincent, and Corbetta, 2005; Damoiseaux et al., 2006; Fox and Raichle, 2007; Smith, Fox, Miller, et al., 2009), including the motor system. Functional neuroimaging of the motor network at rest circumvents the confounds introduced by task difficulty.

Recent findings demonstrate altered resting-state motor connectivity following recovery from stroke (James, Lu, VanMeter, et al., 2009a). When primary or secondary nodes of a brain network are damaged due to a stroke, the effective connectivity of the network suffers (Biswal, Yetkin, Haughton, 1995; He et al., 2007). Consistent diminished effective connectivity across stroke survivors tends to correlate with the patients' motor impairments, while augmented effective connectivity tends to correlate with the patients rehabilitative progress (James et al., 2009a). These findings demonstrate altered resting-state motor connectivity with recovery from stroke, thus supporting the potential use of effective connectivity to assess individual patient's cortical plasticity in response to therapy.

In the current study, we expand upon previous work by evaluating effective connectivity of the motor network at rest in able-bodied participants and stroke survivors with upper limb hemiparesis. We first used exploratory structural equation modeling to derive an optimal model of the motor network in able-bodied participants, then we assessed alterations in that network in stroke survivors. We propose that differences between these two models will reflect how stroke affects motor network connectivity.

2. Methods

2.1 Participants

Fifteen individuals (nine male) who had sustained a single stroke less than 54 months prior to the study and exhibited moderate upper extremity hemiparesis and 12 able-bodied volunteers participated in this study after giving informed consent (Table 1). Stroke latency ranged from 1–54 months before study entry (mean= 10 ± 13.4 months). The stroke survivors age ranged from 42–74 years (60.5 years $\pm$ 10.2; 1 left-handed). The age of the able-bodied people ranged from 27–62 years (41.4 years $\pm$ 15.3; 5 males, 1 left-handed). Able-bodied volunteers were taken as a convenience sample from a separate study and thus were not age-matched with stroke survivors. Healthy volunteers had no history of neurologic or cerebrovascular insult.

Stroke was confirmed by magnetic resonance imaging or computed tomography (CT). The patients exhibited a heterogeneity of stroke type and lesion location (Table 1). Six patients had left hemiparesis resulting from infarct or hemorrhage located in the thalamus, basal ganglia, internal capsule, caudate, and/or precentral gyrus. Seven patients had right hemiparesis due to infarctions of the middle cerebral, pontine or internal carotid arteries.

All stroke survivors but one reported being right-hand dominant prior to the stroke. This was confirmed post-injury via the Edinburgh Inventory. To be included in the study stroke participants had to be at least 18 years old and survived their first stroke within 54 months prior to enrollment. Participants could not be engaged in formal physical rehabilitation programs. Individuals were independent in standing, toilet transfer, and the ability to maintain balance for at least 2 minutes with arm support. Upper extremity movement criteria included the ability to actively extend the affected wrist $\geq 20°$ and extend 2 fingers and thumb at least $10°$ with a motor activity log (MAL) score of less than 2.5 (Uswatte, 2006).

2.2 Clinical Examination

The Motor Activity Log (MAL) is a semi-structured interview for hemiparetic stroke patients to assess the use of their paretic arm and hand (amount of use [AOU] and quality of movement [QOM]) during activities of daily living. Scores range from 0 (never) to 5 (normal) on the QOM scale and 0 (never) to 5 (same as pre-stroke) on the AOU scale.

The Fugl-Meyer Motor Assessment (FM) is a comprehensive assessment of sensation and motor function (reflexes, volitional movement assessment, flexor synergy, extensor synergy, movement combining synergies, movement out of synergy, normal reflex assessment, wrist movement, hand movement, and coordination and speed; Fugl-Meyer, Jaasko, and Leyman, 1975). The upper extremity portion includes a total of 33 items and is scored on a scale of 0–2 (2 points for complete performance of the item, 1 point for partial performance of the item, and 0 for no performance of the item). The total possible score on the upper extremity portion of the FM is 66, with scores of ~33 denoting moderate impairment of the affected upper limb.

The Mini-Mental State Exam (MMSE) is a short, quantitative assessment of the cognitive aspects of mental function. This measure includes 11 questions, split into 2 sections. The first section tests orientation, memory, and attention, while the second section tests the participants' ability to name, follow verbal and written commands, write a sentence spontaneously, and copy a complex polygon. The maximum score on this test is 30, with scores approaching 30 describing normal cognitive function (Folstein, Folstein, and McHugh, 1975). The MMSE was recorded only for the stroke survivors.

2.3 Testing Paradigm

2.3.1 MRI acquisition—Stroke participants underwent one resting-state fMRI (rs-fMRI) scanning session. [TR/TE/FA=2350ms/28ms/90°, 130 time points (~5 min each), resolution=$3 \times 3 \times 3$ mm^3, 35 axial slices) on a Siemens 3.0T Magnetom Trio scanner (Siemens Medical Solutions, USA). Able-bodied volunteers were recruited as a convenience sample from a separate study performed on the same Siemens 3.0T scanner. Consequently, able-body volunteers have a different resting-state fMRI (rs-fMRI) protocol [TR/TE/FA=3000ms/30ms/90°, 140 time points (~7 min each), resolution=$3 \times 3 \times 3$ mm^3, 35 axial slices]. The stroke and able-bodied participant samples also differ in that the rs-fMRI scan for stroke participants was preceded by a motor task involving finger/ thumb opposition, whereas the rs-fMRI scan for able-bodied volunteers was preceded by a cognitive task involving semantic processing of word pairs. For both samples, a 5–7 minute anatomical

scan separated the functional tasks and the resting-state scan, therefore reducing the influence of retained task-related neural activity on the resting state run.

2.4 Data Analyses

2.4.1 Image Processing—Image processing and analysis was performed using SPM5 (www.fil.ion.ucl.ac.uk/spm). After correcting for differences in acquisition times of the different EPI slices (slice-timing correction), all functional datasets were band-pass filtered (0.009-0.08 Hz), motion-corrected (Art Repair software; Mazaika, Hoeft, Glover, and Reiss, 2009), realigned, and unwarped. Art repair software in SPM5 identifies movement related signal in each scan and allows for interpolation of the signal in scans marked with excessive movement. Normalization parameters were derived from segmenting each participant's T1-weighted anatomical brain image. These normalization parameters were then applied to the respective participant's EPI images. Data were spatially smoothed using a Gaussian filter (FWHM= $6 \times 6 \times 6$ mm). Motion parameters were stored and used as nuisance covariates in the correlational seed map analysis. First level models were created for each subject using the extracted time courses of BOLD signal from predefined regions of interest (ROIs) as regressors.

Regions of interest (ROIs) were defined using a mixed seed-based and data-driven correlation mapping procedure to assess functional connectivity between hypothesized regions. The primary motor cortex and superior parietal cortex were selected as seeds. Timecourses for these seeds were derived by extracting the first principle component (first eigenvariate) of each time point per seed using the MarsBar ROI toolbox for SPM5 (Brett et al., 2002). Calculation of the first eigenvariate is derived from computations made in SPM and uses the single value deconvolution (SVD) of the covariance matrix method (FIL Methods Group, 2009). After the 1st eigenvariate was extracted for each time point in the resting state scan, the seed ROI's time course was used as a regressor to produce subject-specific seed correlation maps (Figure 1). Seed regions for each patient were placed in their affected hemisphere (6 left-hemisphere and 7 right-hemisphere strokes), while seeds for all able-bodied participants were placed in the left hemisphere. All further ROIs (described below) were defined and placed based on the suprathreshold regions revealed in the seed correlation maps for each individual and the ROIs used in Solodkin and colleagues model (Solodkin, Hlustik, et al., 2004).

The primary motor area (M1) seed ROI was identified by its distinctive "hand knob" anatomic landmark (James et al., 2009a; Yoursy, Schmid, et al., 1997). A 6-mm radius sphere was placed at each individual's hand knob coordinate (left hemisphere regardless of handedness) and used to generate a correlation seed map. This seed map guided the subject-wise placement of 4 additional ROIs affiliated with the proposed motor execution network: the unaffected (stroke survivors) or right hemisphere (able-bodied participants) M1, the dorsal lateral premotor cortex (pMC) in both hemispheres, and the supplementary motor area (SMA) on the midline of the brain. Because these motor regions have well defined anatomic boundaries, each ROI could be reliably encompassed with a 6mm radius sphere for every participant. The superior parietal area (PAR) seed ROI could not be defined as clearly from anatomy as M1; it was instead defined using the WFU PickAtlas (Maldjian, Laurienti, et al., 2003) according to automated anatomical labeling (AAL) coordinates (Tzourio-Mazoyer et al., 2002). This PAR seed region was included because Solodkin and colleagues (Solodkin, Hlustik, et al., 2004) identified the superior parietal cortex as a hub (similar to M1), of inputs and outputs to frontal regions during execution of upper extremity motor tasks. The PAR seed map guided the placement of 4 additional ROIs for each individual subject: bilateral superior parietal (PAR) and bilateral inferior frontal (IF). These regions were modeled as 10mm radius ROIs because they are functionally more diffuse and

encompass a broader cortical area than the motor system ROIs. One healthy control was excluded from the SEM analysis due to lack of correlation between the right IF and either of the PAR seeds. Importantly, across all participants, individually placed ROIs were consistently either 6 mm or 10 mm in radius for the motor execution or motor control networks, respectively. In addition, each stroke survivor's 5 ROIs were overlaid onto their normalized structural image to ensure that no part of any ROI overlapped the stroke survivor's damaged tissue. No ROIs overlapped any damaged tissue according to the survivor's structural images. Thus, the timecourses extracted from each participant was sampled from existing tissue according to each patient's structural image. For average coordinates for stroke survivor ROIs see table 2.

2.4.2 Structural Equation Modeling (SEM)—Exploratory and confirmatory SEM was conducted using LISREL 8.8 (SSI, Inc.) as previously described (Zhuang, Peltier, Hu, et al., 2005). SEM generates linear equations describing relationships among the variables of interest; in this experiment, the ROI BOLD response timecourses. To visually depict these relationships, paths with arrows indicate the *direction of influence*, while path coefficients reflect the *strength of influence* (unit change in standard deviation denoted by beta score; Figure 1).

For our exploratory adaptation, we constrained permissible paths between ROIs based on a previous confirmatory model of motor execution in the upper limbs of able-bodied volunteers (Solodkin, Hlustik, et al., 2004). We describe the exploratory SEM method as constrained because all of the initial paths were "constrained" to those found previously. It is also possible to perform an "unconstrained" exploratory SEM approach in which all possible paths between ROIs have the potential to be included in the best model. The "unconstrained" approach with the control data was implemented to see if a model similar to our best fitting constrained exploratory model emerged as the best model with all paths open. The unconstrained data-driven approach yielded dozens of statistically indistinguishable models, thus warranting further analyses with the discrete model generated from the constrained exploratory approach. Figure 2A depicts the model that was adapted from Solodkin and colleagues (2004) for constrained exploratory SEM analysis.

All paths were consistent with Solodkin and colleagues' (Solodkin, Hlustik, et al., 2004) motor execution model, with the exception of one additional path. A path from PAR to IF was added for both practical and theoretical reasons. Practical reasons for opening this path include the fact that basic functional connectivity (correlation) between the PAR and IF was observed in the seed-mapping analysis. The correlation between PAR and IF was sufficiently high that the PAR seed could be used to define and localize the IF for each subject in both hemispheres. Inclusion of the IF-PAR path was further supported by the path weight, which survived the exploratory SEM approach with one of the largest path weights and t-scores. Theoretical rationale for inclusion of this path stem from theories that fronto-parietal interactions act as control networks for lower level networks and are non-specific higher order association areas of modalilty-specific systems (Vincent, Khan, and Snyder, 2008).

Two ROIs specified in the Solodkin execution model were not included. The cerebellum was excluded because the fMRI field of view did not consistently capture this region in all subjects. Primary sensory area (S1) was excluded because seed-based correlation maps of M1 and PAR could not appreciably dissociate S1 from M1. Thus, S1 was considered part of the M1 seed to avoid multicollinearity.

ROIs were selected and the constrained model was declared, and the 1st eigenvariate time series for each ROI was extracted (Figure 1). The constrained set of paths was analyzed in

LISREL with the control group concatenated ROI timecourse data using our exploratory SEM approach. This analysis produced a correlation matrix for each possible model from which path coefficients are estimated for the strength and direction of influence of each. The analysis is iterated for all possible models given the constrained set of paths (Figure 1). The exploratory SEM approach produced several thousand possible models that either converged or did not converge. Exclusion and sorting was performed using previously described fit criteria (James, Kelly, Craddock et al., 2009b). Briefly, each model had to include all 5 ROIs and the Akaike Information Criterion (AIC) was computed for each model, where AIC represents a standardized metric of fit across models drawn from the same dataset. The models were initially sorted by their AIC score, and then by their minimum t-score, with the goal of identifying the least significant path for each model. This procedure allowed exclusion of models with several non-significant paths. Finally, the probability of close fit (p-close) of the model was assessed by the root mean squared error of approximation (RMSEA) which should not being significantly different from zero (RMSEA p-close > 0.05).

Reliability and validity of the exploratory model for the healthy controls was assessed using a leave-one-out cross validation. Once the best exploratory model was determined, confirmatory SEM analyses was applied to the model in eleven iterations using the time courses acquired from each healthy control participant. Data from one healthy control subject was left out of the analysis in each iteration.

Once the best constrained exploratory model for the able-bodied controls was determined, a confirmatory SEM was applied to the stroke patient data. This established whether the best model for healthy controls fit the patient data. After running the confirmatory model with the patient data, the two models were compared and any differences evaluated. Any non-significant paths were assessed by evaluating their t-scores in the patient model. Paths with large differences in path weight magnitude between the two models were identified. If patient data adequately fit the healthy control model, then differences in path weight would be slight and all paths would be considered significant.

After determining whether or not the patient data fit the healthy control model, a multi-group confirmatory model was used to test which paths statistically differentiated the groups. The strength of this approach is that paths can be "fixed" between the two models, i.e. path weights can be constrained to be equal for each sample. With all path weights fixed for each sample, if both samples significantly fit the model, then the samples do not significantly differ; on the other hand, if both samples do not significantly fit the model then the samples must differ. If the latter situation arose, paths that potentially differed between samples were 'freed' to differ between samples. In other words, these paths were not fixed to a constant value for each sample, but were allowed to vary between samples. The decision to free paths was guided by the magnitude of the path weight differences between the two groups and any non-significant paths. Paths were iteratively freed until the model that fit both groups with the least number of freed paths was achieved.

To further assess individual difference characteristics of the altered paths, using SPSS 18 (SPSS inc.), Pearson's correlations were analyzed for participant individual difference demographics (age in controls and patients; Fugl-Meyer and time since stroke in patients) and path weights for altered paths.

3. Results

3.1 Able-bodied Control Exploratory Model

The best constrained exploratory model for controls yielded a similar model to the motor execution model previously described by Solodkin and colleagues (Solodkin, Hlustik, et al., 2004), with a few important differences. Figure 1A depicts the theoretical model used in the exploratory approach and Figure 1B depicts the control exploratory model. Two paths left open in the theoretical model did not survive the exploratory SEM process, specifically the IF to SMA and IF to M1 paths. Most of the path weights in our healthy control model are similar to those described by the Solodkin motor execution model. Interestingly, the path from PAR to SMA has an almost identical path weight identified in the Solodkin motor execution model and our resting-state motor network (Motor Exec. path coef. = 0.3–0.6; rs-motor network path coef. =0.51; Figure 2B: PAR to SMA). As will be discussed in detail later, this path was found to be one of two significantly different paths between the healthy control and stroke patient models. The strength of the PAR to M1 path was different between our able-body control data and the Solokin motor execution model (Motor Exec. path coef. = 0.3–0.6; rs-motor network path coef. = 0.16; Figure 2B: M1 to PAR).

All ROIs for the control subjects were confined to the left hemisphere. To verify that there was no difference between the hemispheres, a confirmatory SEM was conducted using the controls right hemisphere data. The control data fit the model confirming no significant differences between hemispheres (RMSEA p-close = 0.08, GFI = 0.988). Reliability of the best exploratory model for the healthy controls was assessed with a leave-one-out method. The models produced in each iteration of the best exploratory model were essentially identical to the model with all participants included (Std. RMR for all models < 0.01).

The best model generated from the exploratory approach for the healthy controls depicts a theoretically sound model, with directional influences from the fronto-parietal circuit connecting to all of the seeded primary motor areas. For clarity, beta weights for path coefficients (b) and t-scores for particular paths are reported in the following format [ROI to ROI = b (t-score)]. The PAR had the most outputs to other areas with 3 strong connections [PAR to pMC=0.34(16.6); PAR to SMA=0.51(23.2); PAR to IF=0.47(12.3)] and one moderately strong connection [PAR to M1=0.16(6.81)] (Figure 2B). The SMA and pMC both exhibited connections to M1. SMA had a strong indirect influence on M1 through the pMC [SMA to pMC=0.48(23.4); pMC to M1=0.50(19.4)] and a moderately strong direct influence on M1 [SMA to M1 = 0.14(5.82)]. The pMC was also connected to the IF with a relatively weak, but significant path [pMC to IF=0.08(3.05)]. The fit indices for this model meet common criteria for a good fit (stRMR < 0.006, RMSEA p-close=1, Model AIC=31.07, AGFI=0.99). In summary, the able-bodied control exploratory model exhibited a theoretically consistent resting-state network similar to a model previously demonstrated in motor execution with additional connectivity between fronto-parietal control cortices and primary motor areas.

3.2 Stroke Patient Confirmatory Model

The application of the healthy control model to the stroke patient group dataset revealed several important differences between the two groups (compare Figure 2B to 1C). First, the PAR to M1 path did not survive to fit in the model, as evidenced by the non-significant t-score and weak path coefficient [PAR to M1=0.01(0.47)] (Figure 2C). Several other paths produced weaker path weights than the healthy control model. Weaker paths included PAR to SMA and pMC to M1 [PAR to SMA=0.35(15.3); pMC to M1=0.37(13.9)] (Figure 2C). Other paths varied only slightly ($\Delta\beta$ <0.1) from the control model. These paths included PAR to IF [0.38(15.8)], PAR to pMC [0.29 (13.7)], pMC to IF [0.17(7.24)], and SMA to

pMC [0.42(19.7)] (Figure 2C). The fit indices for this model met common criteria for a good fit (stRMR < 0.02, RMSEA p-close = 0.99, 39.51, AGFI=0.99). Additionally, the connections between fronto-parietal cortices and primary motor areas appear to be significantly diminished. In summary, the stroke patient confirmatory model exhibited an overall weaker model with good fit to the healthy control exploratory model.

3.3 Multi-Group Confirmatory Model

In order to statistically compare the models derived from each group, a multi-group confirmatory model was created in which paths were initially constrained to a constant value for both groups and then iteratively freed until the model statistically fit both groups. This approach allowed for identification of paths that must change between the groups in order for the confirmatory model to fit both groups. When all paths were fixed between able-bodied and stroke volunteers, the model did not significantly fit either group, indicating that the multi-group model must differ between the groups (Controls Std. RMR = 0.092; Patients Std. RMR = 0.091). The first path freed was the only non-significant path in the patient group; PAR to M1. The exclusion of this path made the multi-group model approach a better fit (Controls Std. RMR = 0.071; Patients Std. RMR = 0.067). The path with the largest difference between the control and patient model was freed next; PAR to SMA. The resulting multi-group model had a good fit with both data sets (Controls Std. RMR = 0.037; Patients Std. RMR = 0.043) (Figure 2D). Importantly, freeing PAR to M1 along with the path with the second greatest difference between control and patient models (pMC to M1) produced a model that did not fit either of the datasets well (Controls Std. RMR = 0.068; Patients Std. RMR = 0.074)]. Thus, the model that significantly fit both data sets with the least number of paths freed between the group models was determined. To summarize, the multi-group model that best fit our datasets was comprised of all paths being held static except for PAR to M1 and PAR to SMA (Controls Std. RMR = 0.037; Patients Std. RMR = 0.043,RMSEA p-close=0.99, Model AIC = 98.5, Control AGFI=0.99, Patient AGFI=0.99) (Figure 2C).

3.4 Individual Differences in Path Coefficients for Important Paths

To gain insight into of the individual differences between the healthy control group and stroke patients group the models for each group were analyzed on an individual subject basis. Path coefficients were extracted for each patient and a dot histogram was plotted. Figures 2a and 2b depict dot histograms for the two critically different paths. Note the values of the group variances in the individual PAR to M1 path weights (Controls M=0.12, SD =0.14; Patients M=0.06, SD =0.27; Figure 3A) and the values of the path weights group averages for PAR to SMA (Controls M=0.50, SD=0.15; Patients M=0.35, SD=0.16; Figure 3B). The path weight distribution in the control group for PAR to M1 is relatively normal with a slight positive skew, while the patient distribution is more variable with several statistical modes. In addition, the variability in the PAR to M1 path of the confirmatory patient model (Figure 2C) and lack of variability in the PAR to M1 path of the exploratory control model (Figure 2B) helps explain the need for this path to vary between the groups in the multi-group model (Figure 2D). Additionally, the PAR to SMA path has reasonably normal distributions with some positive skew in both controls and patients, but the means are significantly shifted between the two groups. This provides further support for path differences between the two groups in the multi-group model analysis.

Pearson's correlations were performed to test whether individual participant characteristics were related to the path weights for the altered paths. In particular, since our experimental groups differed by age, it was especially important to verify that subject's age was not a significant predictor of the path weight value. Indeed, age was not correlated with the path weight for healthy controls or stroke survivors (healthy: PAR to M1, $r(9)=0.38$, $p=0.2$, PAR

to SMA, $r(9)=0.23$, $p=0.5$; stroke: PAR to M1, $r(1)=o.02$, $p=0.9$, or PAR to SMA, $r(11)=-0.15$, $p=0.5$ (Figure 4)). Data for patient 9 was not included in the time since stroke correlation analysis because their time since ictus of stroke was much greater than the remaining cohort (54 months). Stroke survivor Fugl-Meyer scores were not correlated with the path weight for PAR to M1, $r(11)=0.06$, $p=0.8$, or PAR to SMA, $r(11)=-0.06$, $p=0.8$. In addition, the time since ictus of stroke was not correlated with the path weight for PAR to M1, $r(11)=0.04$, $p=0.9$, or PAR to SMA, $r(11)=-0.10$, $p=0.7$.

4. Discussion

This work characterizes important differences between the resting-state motor control network of stroke survivors and healthy participants. The main finding is that specific top-down connections of high-level motor guidance systems to the resting-state motor network are disrupted in stroke survivors relative to healthy individuals. In particular, the pathway from superior parietal cortex (PAR) to primary motor cortex (M1) and supplementary motor cortex (SMA) was diminished in stroke survivors. This finding suggests that motor control deficits following stroke may stem from disconnection between high-order motor guidance systems and the primary motor network. Secondarily, our exploratory SEM approach revealed a model that is consistent with previous network models of motor execution in healthy individuals (Solodkin et al., 2004). Our results have implications for the development of treatments for stroke rehabilitation and the characterization of connectivity between these regions in healthy populations.

4.1.1 Connectivity of fronto-parietal and primary motor networks after stroke

The stroke patient model was specifically distinct from both the theoretical model and the healthy control exploratory model. In particular, the connection of PAR to M1 was not necessary for fitting the healthy control model to the patient data; accounting for only 0.01% of variance observed in M1. Combining both groups in the same model using a stacked model approach, we found that the influence of PAR onto SMA was also significantly different between the two groups.

In one of the first studies to characterize pathological connectivity of stroke patients' motor networks relative to healthy controls (Grefkes, Nowak, et al., 2008a; Grefkes, Eickhoff, et al. 2008b), Grefkes et al. used dynamic causal modeling (DCM) to assess the effective connectivity of M1, pMC, and SMA bilaterally during generation of hand movements in a sample of patients with subcortical stroke. They found pathological interactions both contralaterally and ipsilaterally between these areas in the group with subcortical stroke lesions relative to the healthy control group. In comparing their findings to those of the present study, there are a few interesting points to be noted. First, Grefkes and colleagues suggest that bi-hemispheric dysfunction underlies hand motor disability after stroke. While our study cannot directly address contralateral connections, we did apply the healthy control exploratory model to the right hemisphere of the healthy controls and to time courses extracted from the unaffected hemisphere of the patients. The models derived from our supplementary analyses were similar to the models derived for the left hemisphere in healthy controls, but had some marked alterations similar to the affected hemisphere in our stroke survivor group. In addition, parallel to the data by Grefkes et al. and others (Sharma et al., 2009; Wang et al., 2010), we found diminished ipsilateral connectivity of the PAR to M1 and PAR to SMA in stroke survivors relative to controls. This may suggest a pathological influence of fronto-parietal networks on the path from ipsilesional SMA to contralesional M1 in stroke patients during the recovery period (Grefkes, Nowak, et al., 2008a; Grefkes, Eickhoff, et al. 2008b).

Furthermore, previous work has shown that stroke patients exhibit reduced connectivity between the supplementary motor area and the ipsilesional premotor cortex in both imagined and executed tasks (Sharma et al., 2009). However, during imagery tasks alone, increased coupling was shown between both the ipsilesional prefrontal cortex and premotor cortex, and the ipsilesional prefrontal cortex and supplementary motor area; with associated reduction in coupling between the ipsilesional premotor cortex and supplementary motor area in patients with subcortical stroke (Sharma et al. 2009). The present study did not find a relation between motor network connectivity and motor performance measures, a trend from previous studies shows a pattern of significant reduction in the cortical coupling between the supplementary motor area and ipsilesional primary motor cortex, which appears to be increased with better motor performance (Sharma et al., 2009; James et al., 2009a).

Diminished connectivity following brain insult has been demonstrated in other patient populations. With regard to connectivity between fronto-parietal circuits and primary motor cortex, Guye and colleagues (2003) identified anatomical connectivity through fast-marching tractography (FMT) between the parietal cortex and M1 of a patient with a left precentral lesion. Thus, our findings might be describing the diminution of effective connectivity after cortical or sub-cortical insult. In support of this hypothesis, Rowe and colleagues (2002) present data showing abnormal effective connectivity between IF, pMC, and SMA in patients with Parkinson's disease, which is known for its deficits in motor control due to diminished function of a subcortical circuit (i.e. basal ganglia).

4.1.2 Connection strength variability in stroke survivors

The between-subject variability of PAR to M1 path weights demonstrates an interesting pattern of results, particularly in the stroke patient group. These distributions reveal why PAR is found to reliably influence M1 in healthy subjects but not in stroke patients. In other words, the variability of PAR to M1 path weights across patients makes PAR's influence on M1 negligible in the context of the stroke survivor confirmatory model. Although this idea needs further exploration with more sensitive measures of improvement in upper limb motor function, future rehabilitation interventions could be designed to specifically target (i.e. strengthen) the PAR to M1 path that may lead to more rapid or complete recovery of upper limb function. However, as a caveat, time since stroke was not related to each individual's path weight for this pathological connection.

Also noteworthy, we observed much less overlap in the distributions for the PAR to SMA path weights between patients and controls than for the PAR to M1 path. The PAR to SMA path significantly differed from zero for both control and patient groups, but also significantly differed in magnitude between the groups. This pattern may demonstrate a different phenomenon of diminished connectivity in patients and may not track with rehabilitation; but needs further exploration. Additionally, the difference in magnitude and normal distribution in PAR to SMA path demonstrates why freeing this path in the multi-group confirmatory model allowed for the improved fit of the data to the model.

Interestingly, no relationship was found between patient Fugl-Meyer scores and either of the proposed pathological paths. This finding suggests that the strength of these paths might not be related to individual behavioral outcomes. Although, the lack of correlation between path weights and FM, might also be attributed to the fact that the Fugl-Meyer assesses gross levels of motor function (Uswatte and Taub, 2005), thus lacking the precision to statistically co-vary with the observed alterations in stroke survivor resting state effective connectivity. This negative finding may also be due to large inter-subject variance in the patient's altered path weights, masking the effect of interest. Future studies could examine correlation between the change in altered path weights and motor performance scores from pre-intervention to post-intervention testing sessions.

A potential confound for the observed differences between the control group and the stroke survivors was participant age, since these groups were not age matched. Importantly, no significant correlation was found between age and altered path weights, suggesting group or individual differences in path weights do not stem from the difference in age between individuals or groups (see Figure 4).

In summary, the present study found that the influence top-down attentional control regions (PAR) on primary motor execution regions (M1 and SMA) was altered after stroke, relative to a sample of healthy control participants. These findings contribute to growing evidence from studies of patients with specific lesions to movement related regions, movement disorders, and stroke have altered connectivity between top-down attentional control regions and motor execution regions (Rowe et al., 2002; Guye et al., 2003; Grefkes, Nowak, et al., 2008a; Grefkes, Eickhoff, et al. 2008b; Sharma et al., 2009).

4.2 Connectivity of fronto-parietal and primary motor networks in healthy individuals

In healthy populations, motor task execution and mental imagery involve a direct connection between high-level association areas and primary motor cortices (Solodkin, Hlustik, et al., 2004; Xiong et al. 1999). Using constrained exploratory SEM, our *resting-state* data from healthy controls reveal a model with similar paths and strengths of influence between motor areas and association areas to those previously described by Solodkin et al. (2004).

The SMA, pMC, and M1 are all motor areas consistently included in network models of motor planning and execution. The SMA is known for its involvement in planning the coordination of internally-cued motions (Debaere et al., 2001). The pMC has been implicated in similar functions to the SMA including motor planning and initiation of motor execution (Walsh, Small, and Solodkin, 2008). Primary motor cortex is specifically linked to the representation and execution of motor programs (Solodkin, Hlustik et al., 2004; Grefkes, Eickhoff et al. 2008b). Coordination of inputs and outputs from these regions produce the rich and complex motor behaviors that healthy individuals demonstrate in everyday life. Our resting-state data add supporting evidence that fronto-parietal inputs into these regions guide motor intentions, decision-making, trajectories of movement, and coordination of multiple body parts (Andersen and Cui, 2009). In addition, our comparison of the healthy controls and the stroke survivor models demonstrate that the top -down connections may be important for normal functioning and, as discussed before, appear to be damaged in stroke survivors with moderate levels of impairment in their upper extremity.

Interestingly, several hypothesized connections from IF to M1 and SMA did not survive the exploratory sorting constraints and were therefore not included in the healthy control exploratory model. The exclusion of these paths may be interpreted as less connectivity from IF to M1 in the healthy control model with no other indirect routes of influence between these ROIs. As will be discussed, IF to PAR may constitute a bi-directional path that was not included in the constrained theoretical model for various computational reasons. This characterization may speak to less *direct* influences from IF to primary motor cortices.

4.3 Implications of altered connectivity in stroke for physical and cognitive rehabilitation

Characterizing the deficits in resting-state connectivity of top-down processes in stroke survivors may help researchers to identify neural networks to target with cognitive and physical stroke rehabilitation therapies. Previous studies have described the neural plasticity of motor networks following stroke during task-related activation and resting-state, after rehabilitative therapy (James, et al., 2009a; Small, Hlustik, Noll, Genovese, and Solodkin, 2002). Small and colleagues suggest that cerebellar activation and connectivity predict the outcome of stroke survivors after rehabilitative therapy. Replications of the present study

would likely benefit from an extension of the effective connectivity model to include cerebellar activity, in both able-bodied participants and stroke survivors.

Using a similar adaptation of exploratory SEM, James and colleagues (James, Lu, et al., 2009a) evaluated the predictive power of resting-state motor network connectivity for rehabilitative outcome of stroke survivors. Patients with post-stroke hemiparesis were scanned before and after 3 weeks of focused upper extremity rehabilitation therapy. These patients were also assessed for changes in behavioral and cerebral cortical function. Behaviorally, each patient showed improved upper extremity function after rehabilitation therapy. In all patients, the influence of the pMC in the affected hemisphere (*a*-pMC) upon the pMC of the unaffected hemisphere (*u*-pMC) increased following therapy. The influence of *a*-pMC on M1 of the affected hemisphere (*a*-M1) also increased with therapy for 4 of 5 patients, while the influence of *u*-pMC on *a*-M1 decreased or remained at zero for 4 of 5 patients. Similar to our study, James et al. found altered resting-state motor connectivity in stroke survivors through exploratory SEM, although their comparisons were made in a within-subjects design and a rehabilitative context. In combination with findings from the present study, findings from the preliminary study by James and colleagues suggest that characterizing resting-state networks in stroke patients relative to able-bodied controls is a productive pursuit that informs rehabilitation therapists of cognitive mechanisms that need therapeutic attention following stroke.

Cognitive and physical therapies are prevalent in the treatment of motor impairment following stroke. The main finding of the present study suggests a fundamental disconnection between fronto-parietal association areas and primary motor areas in people with motor impairment following stroke. The fronto-parietal circuit has been proposed to perform the selection, preparation, and execution of movements through proprioceptive, visual, attentional, and other information, like mental representations (Wise, Boussaoud, Johnson, and Caminiti, 1997). Generation of spatial representations by integrating different sensory modalities during goal-directed movements has been demonstrated by the functional interaction between the superior parietal and frontal cortices, in both macaques and humans (Fogassi, et al., 2005; Wenderoth, Toni, Bedeleem, Debaere, and Swinnen, 2006). In this perspective, Fogassi and Luppino (Fogassi, 2005) describe the parietal cortex as part of the motor system whose role is to provide a neural mechanism for higher-order cognitive motor functions, like planning and control. Selection of cognitive and physical therapies may be informed by convergent studies of connectivity and interactions between fronto-parietal guidance systems and primary motor execution networks in both healthy individuals and patients suffering from deficits in motor function due to brain damage (e.g. stroke, Parkinsons disease, etc.)

4.4 Caveats

While creating and describing models of effective connectivity is an appropriate method to characterize the influences among neural networks, it is import to bear in mind that all models are oversimplifications of the actual phenomenon of study. For example, we chose to allow PAR to drive IF so that the model could be solved recursively. Freeing IF to potentially drive PAR would have resulted in a non-recursive model (one which cannot be solved recursively), which are computationally difficult to solve and could easily become computationally unstable (McIntosh and Gonzalez-Lima, 1994). In reality, influences between PAR and IF may be bidirectional. To resolve this issue, we repeated the exploratory modeling while permitting bidirectional paths between IF and PAR and unidirectional paths from IF to PAR. Despite the altered directionality between IF and PAR in the resulting models, PAR to M1 and PAR to SMA still discriminated the healthy subjects and patients. To conclude, our model cannot sufficiently comment on the direction of influence between PAR and IF, but this does not invalidate our results.

Another important caveat of this study is the variability in lesion location in our sample of stroke survivors (Table 1). Previous studies of connectivity and activity in the motor execution network of stroke patients have noted consistent decreases or connectivity deficits in and between regions known to govern motor execution. First, the activity of motor execution regions (e.g. SMA) after stroke has been shown to vary as a function individual differences in recovery status and sensory discrimination (Carey et al., 2006; Carey et al. 2011). For instance, good recovery status was associated with relatively normal patterns of SMA activity, whereas poor recovery status after stroke was associated with consistent reductions in SMA activity during motor execution (Carey et al., 2006). In addition, Ward et al. (2003) found consistent decreases in activity of several motor execution and control network regions (M1, PAR, SMA) following stroke. In terms of decreases in connectivity of motor execution and control regions, Grefkes et al. (2007) showed consistent disturbances in the intrinsic neural coupling between ipsilesional SMA and M1 across patients with variable lesion locations. In all of these studies the stroke locations were considerably variable, yet they all show consistent group effects of decreased activity or diminished connectivity between areas similar to the network modeled in our study. It is possible that consistent changes in the neural connectivity between regions governing motor execution and motor control following stroke is related to this effect of decreased activity in motor regions. Although some studies have found consistent stroke related deficits in brain activation and effective connectivity, the processes that lead to consistent deficits in connectivity across patient samples with variable lesion locations are not well understood and warrant more research.

Several critiques can be made on the convenience sampling approach. Able-bodied participants were acquired from an existing dataset, and therefore were not demographically matched to the stroke patient group. Additionally, the resting-state scans were preceded by a motor task in patients and a language task in able-bodied participants. Waites et al. (2005) have suggested that prior cognitive tasks can have a priming effect on recruited regions, and thereby elicit greater connectivity of these regions in subsequent resting-state scans. However, they also report that the extent and magnitude of priming varied considerably across individuals, and the group connectivity networks were largely consistent irrespective of preceding task. The debate on "carry-through" effects of task on resting-state imaging remains unresolved and is beyond the scope of this paper. Finally, another potential confound in our study could be the slight differences in the scanning parameters, although attempts were made to reduce any effects of these differences.

5. Conclusion

In summary, the present study found a disruption in the influence of a region implicated in top-down attentional control (Corbetta and Shulman, 2002) on primary motor regions in stroke survivors with heterogeneous stroke locations, during the resting-state. This finding supported our hypotheses that important connections between regions implicated in top-down attentional control (PAR and IF) systems and primary motor systems would show diminished connectivity in stroke survivors before rehabilitative therapy, while maintaining their influence in healthy controls during the resting state. Importantly, none of the stroke locations directly corresponded to any of the functionally correlated ROIs used to generate structural equation models of effective connectivity. This allows conclusions to be made about functional damage to the paths between existing structures and not about the direct anatomical damage to a region of interest. To our knowledge, this is the first report demonstrating altered resting state fMRI effective connectivity between fronto-parietal control systems and the primary motor network in stroke survivors with moderate upper limb impairment. This finding suggests that the inability of high-level control systems to influence motor control may significantly contribute to upper limb hemiparesis in stroke

survivors. Individual differences in these disruptions indicate that the functional reorganization in resting-state motor networks following a stroke is quite idiosyncratic, with large between-subject variability. With evidence of damage to pathways for motor guidance in stroke, it is necessary for future studies to determine the relationship between such alterations and the patient's degree of clinical impairment. Determining whether rehabilitative therapy changes effective connectivity between these important brain regions is an important next step in learning how to improve the therapeutic intervention. Future research should evaluate the contributions of bottom-up and top-down cognitive rehabilitation strategies in stroke survivors. Resting-state fMRI and resting-state connectivity analyses appear to be promising methodologies for assessing the effects of stroke on neural networks and the plasticity of these networks after intervention.

Acknowledgments

REFERENCE

Andersen RA, Cui H. Intention, Action Planning, and Decision Making in Parietal-Frontal Circuits. Neuron. 2009; 63(5):568–583. [PubMed: 19755101]

Biswal B, Yetkin FZ, Haughton VM, Hyde JS. Functional connectivity in the motor cortex of resting human brain using echo-planar MRI. Magn Reson Med. 1995; 34(4):537–541. [PubMed: 8524021]

Brett, M.; Anton, J-L.; Valabregue, R.; Poline, J-B. Region of interest analysis using an SPM toolbox [abstract]; Presented at the 8th International Conference on Functional Mapping of the Human Brain; Sendai, Japan. 2002.

Buchel C, Friston KJ. Modulation of connectivity in visual pathways by attention: cortical interactions evaluated with structural equation modelling and fMRI. Cereb Cortex. 1997; 7:768–778. [PubMed: 9408041]

Buchel C, Coull JT, Friston KJ. The predictive value of changes in effective connectivity for human learning. Science. 1999; 283:1538–1541. [PubMed: 10066177]

Cabeza R, Nyberg L. Imaging cognition II: an empirical review of 275 PET and fMRI studies. J. Cog. Neurosci. 2000; 12(1):1–47.

Carey LM, Abbott DF, Egan GF, O'Keefe GJ, Jackson GD, Bernhardt J, Donnan GA. Evolution of Brain Activation with Good and Poor Motor Recovery after Stroke. Neurorehabil Neural Repair. 2006; 20:24–41. [PubMed: 16467276]

Carey LM, Abbott DF, Harvey MR, Puce A, Seitz JR, Donnan GA. Relationship Between Touch Impairment and Brain Activation After Lesions of Subcortical and Cortical Somatosensory Regions. Neurorehabil Neural Repair. 2011; 25:443–457. [PubMed: 21382887]

Centers for Disease Control and Prevention (CDC). Prevalence of disabilities and associated health conditions among adults: United States, 1999. MMWR Morb Mortal Wkly Rep. 2001; 150:120–125.

Corbetta M, Shulman GL. Control of goal-directed and stimulus-driven attention in the brain. Nat Rev Neurosci. 2002; 3:201–215. [PubMed: 11994752]

Craggs JG, Price DD, Verne GN, Perlstein WM, Robinsona MM. Functional brain interactions that serve cognitive-affective processing during pain and placebo analgesia. Neuroimage. 2007; 38:720–729. [PubMed: 17904390]

Damoiseaux JS, Rombouts SA, Barkhof F, Scheltens P, Stam CJ, Smith SM, Beckmann CF. Consistent resting-state networks across healthy subjects. PNAS. 2006; 103:13848–13853. [PubMed: 16945915]

Debaere F, Swinnen SP, Sunaert S, Van Hecke P, et al. Brain areas involved in interlimb coordination: a distributed network. Neuroimage. 2001; 14:947–958. [PubMed: 11697927]

Deiber MP, Passingham RE, Colebatch JG, Friston KJ, Nixon PD, Frackowiak RS. Cortical areas and the selection of movement: a study with positron emission tomography. Exp Brain Res. 1991; 84:393–402. [PubMed: 2065746]

Fogassi L, Ferrari PF, Gesierich B, Rozzi S, Chersi F, Rizzolatti G. Parietal Lobe: From Action Organization to Intention Understanding. Science. 2005; 308(5722):662–667. [PubMed: 15860620]

Folstein MF, Folstein SE, McHugh PR. "Mini-mental state": A practical method for grading the cognitive state of patients for the clinician. J.Psychiatric Research. 1975; 12(3):189–198.

Fox MD, Snyder AZ, Vincent JL, Corbetta M, Van Essen DC, Raichle ME. The human brain is intrinsically organized into dynamic, anticorrelated functional networks. PNAS. 2005; 102(27): 9673–9678. [PubMed: 15976020]

Fox MD, Raichle ME. Spontaneous fluctuations in brain activity observed with functional magnetic resonance imaging. Nat. Rev. Neurosci. 2007; 8:700–711. [PubMed: 17704812]

Friston KJ, Harrison L, Penny W. Dynamic causal modelling. Neuroimage. 2003; 19:1273–1302. [PubMed: 12948688]

Fugl-Meyer AR, Jaasko L, Leyman I, Olsson S, Steglind S. The post-stroke hemiplegic patient. 1. a method for evaluation of physical performance. Scand J Rehabil Med. 1975; 7(1):13–31. [PubMed: 1135616]

Grefkes C, Nowak DA, Eickhoff SB, Dafotakis M, Küst J, Karbe H, et al. Cortical connectivity after subcortical stroke assessed with functional magnetic resonance imaging. Annals of Neurology. 2008a; 63(2):236–246. [PubMed: 17896791]

Grefkes C, Eickhoff SB, Nowak DA, Dafotakis M, Fink GR. Dynamic intra- and interhemispheric interactions during unilateral and bilateral hand movements assessed with fMRI and DCM. Neuroimage. 2008b; 41:1382–1394. [PubMed: 18486490]

Guye M, Parker GJM, Symms M, Boulby P, Wheeler-Kingshott CAM, Salek-Haddadi A, Barker GJ, Duncan JS. Combined functional MRI and tractography to demonstrate the connectivity of the human primary motor cortex in vivo. Neuroimage. 2003; 19(4):1349–1360. [PubMed: 12948693]

He AG, Tan LH, Tang Y, James GA, Wright P, Eckert MA, Fox PT, Liu Y. Modulation of neural connectivity during tongue movement and reading. Hum Brain Mapp. 2003; 18:222–232. [PubMed: 12599281]

He BJ, Snyder AZ, Vincent JL, Epstein A, Shulman GL, Corbetta M. Breakdown of functional connectivity in frontoparietal networks underlies behavioral deficits in spatial neglect. Neuron. 2007; 53(6):905–918. [PubMed: 17359924]

James G, Lu Z-L, VanMeter J, Sathian K, Sathian MDP, Hu X, et al. Changes in Resting State Effective Connectivity in the Motor Network Following Rehabilitation of Upper Extremity Poststroke Paresis. Topics in Stroke Rehabilitation. 2009a; 16(4):270–281. [PubMed: 19740732]

James GA, Kelley ME, Craddock RC, Holzheimer PE, Dunlop B, Nemeroff C, Mayberg HS, Hu XP. Exploratory structural equation modeling of resting-state fMRI: applicability of group models to individual subjects. Neuroimage. 2009b; 45:778–787. [PubMed: 19162206]

Xiong J, Parsons LM, Gao J, Fox PT. Interregional Connectivity to Primary Motor Cortex Revealed Using MRI Resting State Images. Human Brain Mapping. 1999; 156:151–156. [PubMed: 10524607]

Liu Y, Ramnani N, Toni I, Passingham RE, Haggard P. The cerebellum and parietal cortex play a specific role in coordination: a PET study. Neuroimage. 2001; 14:899–911. [PubMed: 11554809]

Maldjian JA, Laurienti PJ, Kraft RA, Burdette JH. An automated method for neuroanatomic and cytoarchitectonic atlas-based interrogation of fMRI data sets. NeuroImage. 2003; 19(3):1233–1239. [PubMed: 12880848]

Mazaika P, Hoeft F, Glover GH, Reiss AL. Methods and Software for fMRI Analysis for Clinical Subjects, poster presented at Human Brain Mapping. 2009

McIntosh AR, Gonzalez-Lima F. Network interactions among limbic cortices, basal forebrain, and cerebellum differentiate a tone conditioned as a Pavlovian excitor or inhibitor: fluorodeoxyglucose

mapping and covariance structural modeling. J Neurophysiol. 1994; 72(4):1717–1733. [PubMed: 7823097]

Miller EK. The prefrontal cortex: complex neural properties for complex behavior. Neuron. 1999; 22:15–17. [PubMed: 10027284]

Miyachi S, Hikosaka O, Miyashita K, Kárádi Z, Rand MK. Differential roles of monkey striatum in learning of sequential hand movements. Exp. Brain Research. 1997; 115:1–5.

Passingham, RE. From where does motor cortex get its instructions?. In: Wise, S., editor. Neural and Behavioral Approaches to Higher Brain Function. New York: Wiley; 1987.

Rijntjes M, Buechel C, Kiebel S, Weiller C. Multiple somatotopic representations in the human cerebellum. Neuroreport. 1999; 10:3653–3658. [PubMed: 10619661]

Rosamond W, Flegal K, Friday G, et al. Heart disease and stroke statistics-2007 update: a report from the American Heart Association Statistics Committee and Stroke Statistics Subcommittee. Circulation. 2007; 115(5):69–171.

Rowe J, Stephan KE, Friston K, Frackowiak R, Lees A, Passingham R. Attention to action in Parkinson's disease: Impaired effective connectivity among frontal cortical regions. Brain. 2002; 125(2):276–289. [PubMed: 11844728]

Sharma N, Baron JC, Rowe JB. Motor imagery after stroke: relating outcome to motor network connectivity. Annals of neurology. 2009; 66(5):604–616. [PubMed: 19938103]

Small SL, Hlustik P, Noll DC, Genovese C, Solodkin A. Cerebellar hemispheric activation ipsilateral to the paretic hand correlates with functional recovery after stroke. Brain. 2002; 125(7):1544–1557. [PubMed: 12077004]

Smith SM, Fox PT, Miller KL, Glahn DC, Fox PM, Mackay CE, Filippini N, Watkins KE, Toro R, Laird AR, Beckmann CF. Correspondence of the brain's functional architecture during activation and rest. PNAS. 2009; 106(31):13040–13045. [PubMed: 19620724]

Solodkin A, Hlustik P, Chen EE, Small SL. Fine modulation in network activation during motor execution and motor imagery. Cereb Cortex. 2004; 14(11):1246–1255. [PubMed: 15166100]

Tanji J. The supplementary motor area in the cerebral cortex. Neurosci. Research. 1996; 19:251–268.

Toni I, Krams M, Turner R, Passingham RE. The time course of changes during motor sequence learning: a whole-brain fMRI study. Neuroimage. 1998; 8:50–61. [PubMed: 9698575]

Tzourio-Mazoyer N, Landeau B, Papathanassiou D, Crivello F, Etard O, Delcroix N, et al. Automated anatomical labeling of activations in SPM using a macroscopic anatomical parcellation of the MNI MRI single-subject brain. NeuroImage. 2002; 15(1):273–289. [PubMed: 11771995]

Uswatte G, Taub E. Implications of the learned nonuse formulation for measuring rehabilitation outcomes: lessons from constraint-induced movement therapy. Rehabil. Psychol. 2005; 50:34–42.

Uswatte G, Taub E, Morris D, Light K, Thompson PA. The Motor Activity Log-28: assessing daily use of the hemiparetic arm after stroke. Neurology. 2006; 67(7):1189–1194. [PubMed: 17030751]

Vincent JL, Kahn I, Snyder AZ, Raichle ME, Buckner RL. Evidence for a Frontoparietal Control System Revealed by Intrinsic Functional Connectivity. J. Neurophysio. 2008; 100(6):3328–3342.

Walsh RR, Small SL, Chen EE, Solodkin A. NeuroImage Network activation during bimanual movements in humans. NeuroImage. 2008; 43:540–553. [PubMed: 18718872]

Waites AB, Stanislavsky A, Abbott DF, Jackson GD. Effect of prior cognitive state on resting state networks measured with functional connectivity. Human brain mapping. 2005; 24(1):59–68. [PubMed: 15382248]

Wang L, Yu C, Chen H, Qin W, He Y, Fan F, et al. Dynamic functional reorganization of the motor execution network after stroke. Brain. 2010; 133:1224–1238. [PubMed: 20354002]

Ward NS, Brown MM, Thompson AJ, Frackowiak RSJ. Neural correlates of motor recovery after stroke: a longitudinal fMRI study. Brain. 2003; 126:1–21.

Wenderoth N, Toni I, Bedeleem S, Debaere F, Swinnen SP. Information processing in human parieto-frontal circuits during goal-directed bimanual movements. NeuroImage. 2006; 31(1):264–278. [PubMed: 16466679]

Wise SP, Boussaoud D, Johnson PB, Caminiti R. Premotor and Parietal Cortex: Corticocortical Connectivity and Combinatorial Computations. Annual Review of Neuroscience. 1997; 20(1):25–42.

Yousry TA, Schmid UD, Alkadhi H, et al. Localization of the motor hand area to a knob on the precentral gyrus. A new landmark. Brain. 1997; 120:141–157. [PubMed: 9055804]

Zhuang J, LaConte S, Peltier S, Zhang K, Hu X. Connectivity exploration with structural equation modeling: an fMRI study of bimanual motor coordination. NeuroImage. 2005; 25(2) 462–447.
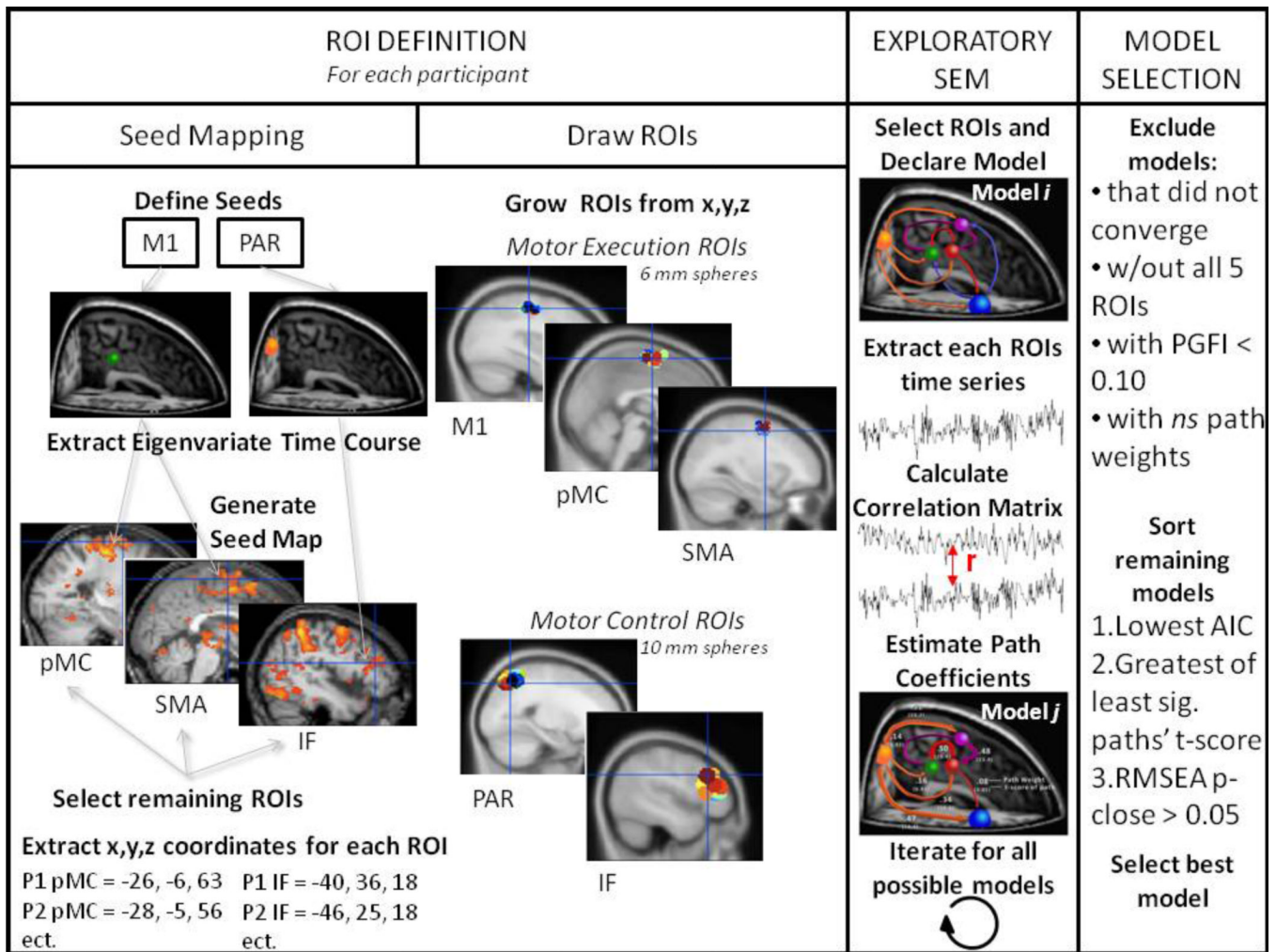
Figure 1.
Illustration of data processing and analysis. Please see text for a detailed description of the preprocessing procedure. ROI definition was performed for each participant individually to account for variability in functional location of each ROI. Example seed maps for the affected or left hemisphere ROI are depicted under seed mapping. Under draw ROIs, the colored sphere for each participant and each ROI are overlaid on a template brain. See table 2 for average coordinates for each of the modeled ROIs. M1, pMC, and SMA were defined with 6 mm spherical ROIs. PAR and IF were defined with 10 mm spherical ROIs. For the exploratory SEM steps, the ROIs and model was based on a previously SEM derived model of motor execution (Solodkin et al., 2004). As with the seed mapping the 1st eigenvariate time course was extracted for each of the ROIs in the model. Correlations matrices and path coefficients were estimated in LISREL and then this process was iterated for all possible models in a MATLAB script. There were 3 basic steps to model selection. First poor models which fit one of the criteria above were excluded. Then the remaining models were sorted according to the 3 sorting criteria. Finally, the best model according to these sorting criteria was selected. Abbreviations: ROI=Region of Interest, M1=primary motor cortex, PAR=superior parietal, pMC=pre-motor cortex, SMA=supplementary motor area, IF=inferior frontal cortex, w/out=without, PGFI=parsimonious goodness of fit index, AIC=akaike information criterion, RMSEA=root mean square error of approximation.
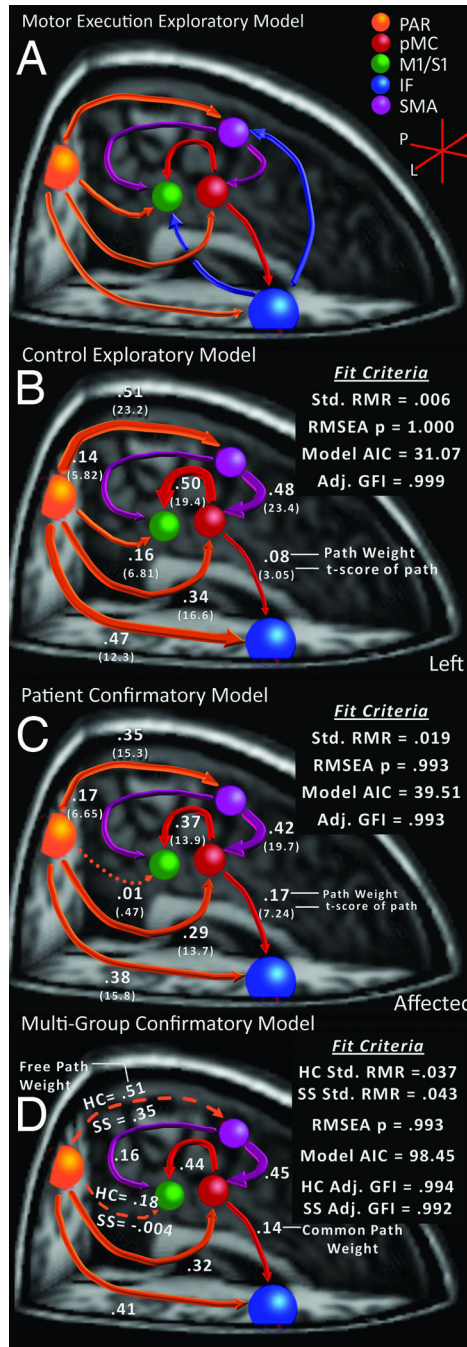
Figure 2.
Resting-state motor network for healthy controls, patients, and a multi-group comparison model. A) The theoretically constrained exploratory SEM based on Solodkin and colleagues (2004). We included the PAR to IF path in addition to Solodkin's ROIs for practical data-driven and theoretical reasons. B) Exploratory SEM for the control group. C) Confirmatory SEM for the patient group. D) Confirmatory multi-group model for comparison of control and patients. Above each path is the path coefficient for that path. Below each path in parentheses is the t-score for that path. Dotted lines signify non-significant paths or paths that are significantly different between groups. Note that the line thickness corresponds to the weight of this particular path. The differences between the constrained exploratory

model and the paths that survived the exploratory control model are striking. This figure also depicts the lack of connection from PAR to M1 in the patient confirmatory model and the significant difference in the PAR to M1 and PAR to SMA paths between the two groups. ROI labels: M1 = Primary Motor Cortex (encompassing S1), pMC = Pre-Motor Cortex, SMA = Supplementary Motor Area, PAR = Superior Parietal Cortex, IF=Inferior Frontal Cortex.
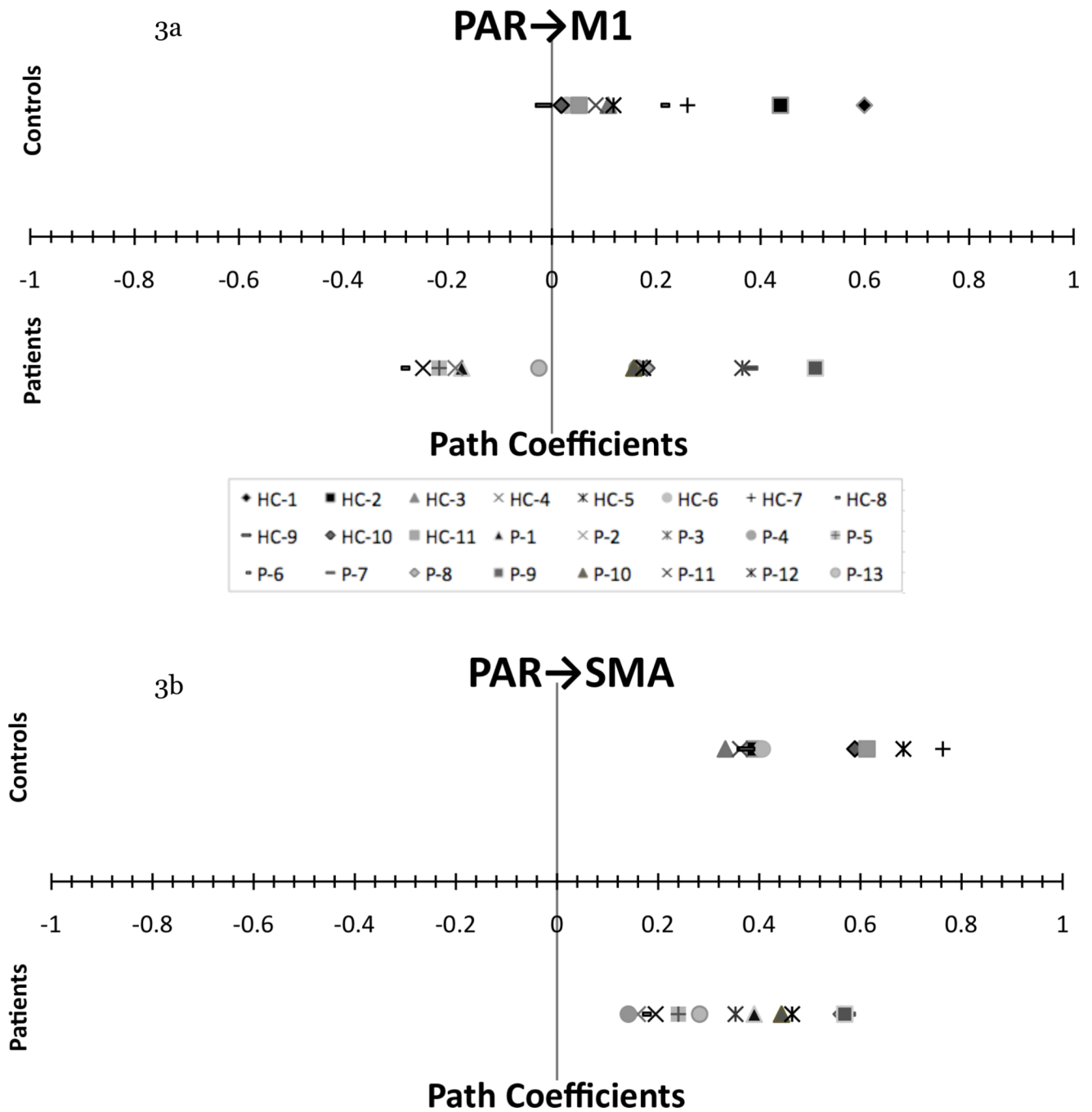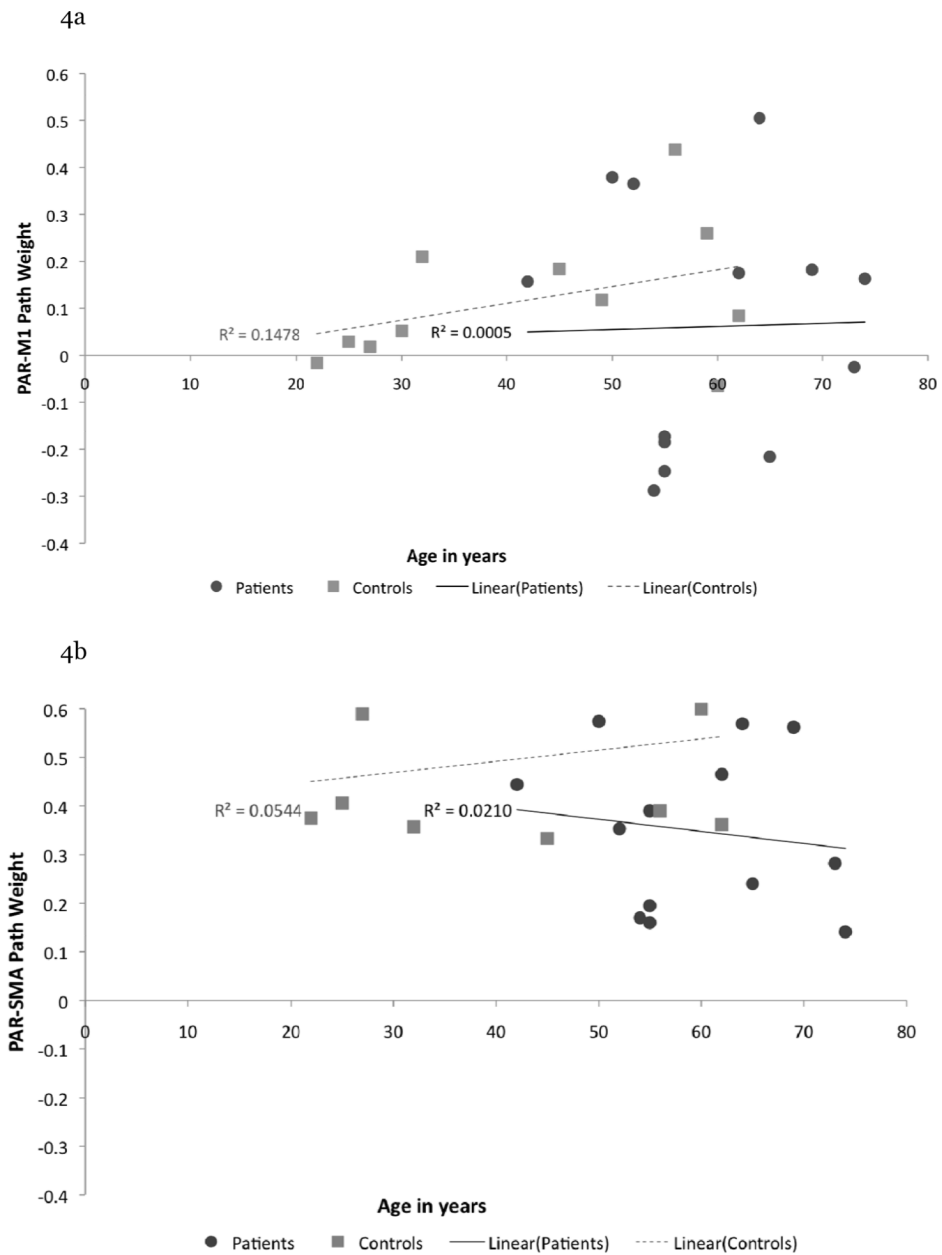
Figure 3.
Dot histograms of the individual subject path weights for controls and patients. a.) Dot histogram of individual subjects' path weights for PAR to M1 path. Notice the relatively normal distribution in the control patients, while the distribution for the patients is quite variable and somewhat bimodal. b.) Dot histogram of individual subjects' path weights for PAR to SMA path. Notice the apparent difference between the magnitude and mean of control and patient distributions.

4a

4b

1

Figure 4.
Scatter plots of participant age (ordinate) and path weight (abscissa) for proposed altered connections. a.) Scatter plot of participant age and PAR→M1 path weight b.) Scatter plot of participant age and PAR→SMA path weight. Note that no significant correlation is found between patient age and path weight for either proposed altered connections. R^2 represents the square of the sample correlation coefficients. The solid line represents the patient line of best fit. The dashed line represents the control line of best fit. The filled circles represent individual patients and the filled squares represent individual control participants.

Table 1

Characteristics of the stroke group.

Subject	Age (years)	Sex	MMSE	Post stroke (months)	Stroke location	Fugl-Meyer Total
1	55	Female	30	5	L Thal. Hem.	27
2	55	Male	27	1	L Basal ganglia	52
3	52	Male	24	8	R cingulate gyrus infarct	40
4	74	Female	30	9	R caudateinfarct	32
5	65	Female	28	7	L caudate infarct	28
6	54	Male	27	11	R putamen hem.	29
7	50	Male	30	5	R lacunar infarct (globus pallidus)	40
8	69	Female	28	8	R motor cortex infarct	34
9	64	Male	28	54	R basal ganglia, thalamic Hem.	30
10	42	Male	30	5	R pontine infarct	46
11	55	Male	28	7	L internal capsule	42
12	62	Male	28	7	L thalamic hem.	36
13	73	Male	28	5	L pontomedullary	31

Table 2

Average centroid coordinate for stroke survivor ROIs

Region of Interest	Hemi	Mean MNI centroid coordinate		
		x	y	z
Motor Execution Circuit				
Primary Motor Area (M1)	L	−33.0	−19.8	52.1
	R	35.7	−18.1	52.0
Pre-Motor Cortex (pMC)	L	−34.3	−1.4	55.8
	R	35.1	0.1	54.9
Suppl. Motor Area (SMA)	Midline	0.0	−4.2	64.7
Fronto-Parietal Motor Control Circuit				
Superior Parietal Cortex (PAR)	L	−22.2	−63.7	55.8
	R	23.9	−63.1	54.7
Inferior Frontal Cortex (IF)	L	−45.4	32.2	18.3
	R	48.5	34.1	15.1